Internal Friction and Nonequilibrium Unfolding of Polymeric Globules

Internal Friction and Nonequilibrium Unfolding of Polymeric Globules

Alfredo Alexander-Katz,[1,2] Hirofumi Wada,[2,3] and Roland R. Netz[2]

[1]*Department of Materials Science and Engineering, MIT, Cambridge, Massachusetts 02139, USA*
[2]*Physics Department, Technical University Munich, 85748 Garching, Germany*
[3]*Yukawa Institute for Theoretical Physics, Kyoto University, Kyoto 606-8502, Japan*

(Received 26 October 2007; published 8 July 2009)

The stretching response of a single collapsed homopolymer is studied using Brownian dynamic simulations. The irreversibly dissipated work is found to be dominated by internal friction effects below the collapse temperature, and the internal viscosity grows exponentially with the effective cohesive strength between monomers. These results explain friction effects of globular DNA and are relevant for dissipation at intermediate stages of protein folding.

DOI: 10.1103/PhysRevLett.103.028102 PACS numbers: 87.15.−v, 62.40.+i, 82.37.−j

Conformational kinetics are crucial for the function of biopolymers: e.g., the muscle protein titin unfolds at a particular loading force in a highly dissipative manner, irreversibly converting most of the mechanical work into heat [1], while in myoglobin ligand dissociation induces a global conformational change of the protein [2–4]. Such transitions involve spatial protein reorganization, and thus internal dissipation mechanisms on different conformational levels in addition to solvent viscosity become important in determining the dynamic response to a given stimulus.

Different contributions to internal polymeric friction have experimentally been distinguished [5]: On the smallest length scale are conformational molecular transitions involving torsional bond degrees of freedom [6,7]. For polymer solutions above the overlap concentration or for polymers in confined geometries, entanglement effects become important and contribute significantly [8]. Finally, for collapsed polymers or folded proteins, the continuous breakage and reformation of cohesive bonds gives rise to an extra contribution to the viscosity inside a globule [9,10]. The significant consequence particularly for protein science is that internal friction may dictate the rate of conformational kinetics and thus protein function dynamics. In all of these experimental studies, care is taken to isolate internal friction effects from the (in the present context uninteresting) hydrodynamic drag of the solvent by, for example, variation of the solvent viscosity [7].

Coarse-grained stochastic models that involve activated hopping events in smooth and idealized energy landscapes nicely explain experimental titin unfolding force curves and provide insight into the dissipation mechanism involving two-step unfolding [11]. A different mechanism is expected for globular homopolymers, proteins in the molten globular state [12], and some disordered intermediates that occur during conformational protein transformations [13]. Here many near-optimal competing states exist, the energy landscape is rough, and structural changes occur gradually through a whole spectrum of intermediate states [14,15]. Many cohesive bonds are broken and reformed repeatedly during unfolding, and the concept of an internal effective viscosity naturally arises [9,10]. There have been quite a few simulation studies on the forced unfolding of bead-spring models for proteins [16] and globular polymers [17,18], but the concept of an internal viscosity has not been applied to models including chain conformational fluctuations.

In this Letter, we study the rate-dependent forced unfolding of a flexible homopolymer model above and below the collapse transition using Brownian dynamic simulations. By measuring the dissipated work, we characterize the internal viscosity at the single molecule level. In particular, we find that the internal viscosity decreases as one lowers the monomer cohesive strength and vanishes at the collapse point. This behavior is surprisingly well captured by a simple stochastic theory that mimics strand-on-strand friction by the forced motion of a single particle in a corrugated potential landscape [14] and also matches well experimental results for the forced unfolding of collapsed DNA [10]. Our results demonstrate how small-scale conformational barriers in highly confined globular chains give rise to an effectively increased internal viscosity. Furthermore, our approach is quite general as it is based on the response of a complex medium (the polymer) to an external force from which the friction coefficient can be obtained in a straightforward way. This approach can, in principle, be used to access rate-dependent dissipative mechanisms that are otherwise inaccessible and sets the stage for tackling more complicated models involving sequence-specific effects.

We model the homopolymer by N freely jointed beads of radius a interacting through a potential U. The position $\mathbf{r}_i$ of the ith bead obeys the Langevin equation $\partial \mathbf{r}_i/\partial t = -\mu_0 \nabla_{\mathbf{r}_i} U[\{\mathbf{r}_N\}] + \sqrt{\mu_0}\boldsymbol{\xi}_i(t)$, where $\mu_0 = 1/(6\pi\eta_0 a)$ is the Stokes mobility and η_0 the solvent viscosity. Hydrodynamic interactions are neglected since we are

interested in friction generated by monomer interactions. The vector random force $\boldsymbol{\xi}_i$ satisfies $\langle \boldsymbol{\xi}_i(t)\boldsymbol{\xi}_j(t')\rangle = 2k_BT\mathbf{1}\delta_{ij}\delta(t-t')$, where k_BT denotes the thermal energy and $\mathbf{1}$ is the unit matrix. The potential energy U is written as $U = U_{\rm el} + U_{\rm LJ} + U_{\rm str}$. The elastic term $U_{\rm el} = (\kappa/2)\times \sum_{i=1}^{N-1}(r_{ii+1} - 2a)^2$, with $\kappa = 200k_BT/a^2$ and $r_{ij} = |\mathbf{r}_i - \mathbf{r}_j|$, controls chain stretching. The Lennard-Jones potential $U_{\rm LJ} = \epsilon\sum_{ij}[(2a/r_{ij})^{12} - 2(2a/r_{ij})^6]$ describes monomer cohesion: Increasing ϵ drives the polymer from the swollen to the collapsed state [17]. The unfolding/refolding is enforced by two symmetrically moving harmonic springs $U_{\rm str} = (\kappa/2)\{[\mathbf{r}_1 + \mathbf{R}(t)]^2 + [\mathbf{r}_N - \mathbf{R}(t)]^2\}$ connected to the end beads. We periodically change $\mathbf{R}(t)$ between $\mathbf{R} = \hat{\mathbf{x}}L/20$ and $\mathbf{R} = \hat{\mathbf{x}}L/2$ at velocity v, thereby changing the polymer end-to-end distance between $|\mathbf{r}_1 - \mathbf{r}_N| = L/10$ and $|\mathbf{r}_1 - \mathbf{r}_N| = L$, where $L = 2aN$ is the chain contour length. The cycle is repeated at least 10 times, over which force traces are averaged separately for the stretch and relax parts. For the numerical integration we discretize the Langevin equation with a time step Δt. We rescale distance by the bead radius a, time by the bare monomer diffusion time $\tau = a^2/(\mu_0 k_BT)$, and energies by k_BT. Our dimensionless parameters are thus the rescaled pulling velocity $\tilde{v} = v\tau/a$, the Langevin time step $\Delta\tilde{t} = \Delta t/\tau = 2\times 10^{-4}$, and the cohesive strength $\tilde{\epsilon} = \epsilon/k_BT$.

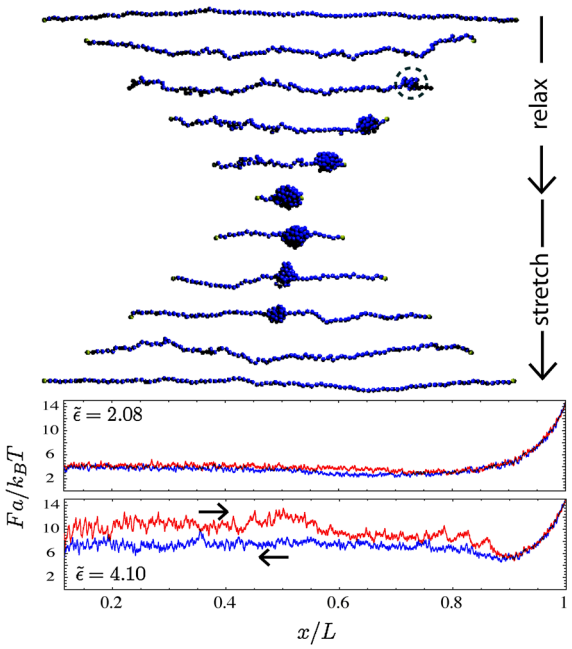

FIG. 1 (color online). Top: Snapshots of a relax-stretch cycle for a polymer with $N = 100$ monomers and cohesive strength $\tilde{\epsilon} = \epsilon/k_BT = 2.08$. The stills are taken at equally spaced times and span a whole cycle; i.e., the first and the final snapshots correspond to fully elongated configurations. Bottom: Force-extension traces for $\tilde{\epsilon} = 2.08$ and 4.1. The blue and red curves correspond to relaxation and stretching, respectively, as indicated in the lowest panel. The stretching velocity in all plots is set to $\tilde{v} = v\tau/a = 0.0045$.

Typical force-extension traces, averaged over 10 relax-stretch cycles, are shown in Fig. 1 for two different cohesive strengths $\tilde{\epsilon}$ at velocity $\tilde{v} = 0.0045$, together with snapshots for $\tilde{\epsilon} = 2.08$. For $\tilde{\epsilon} = 2.08$, the hysteresis between the relax and stretch force traces is small, indicating quasiequilibrium and suggesting that the cycle time $T \simeq L/v$ is larger than the globule relaxation time. For the higher cohesion $\tilde{\epsilon} = 4.1$, hysteresis is noticed; in addition, a force dip at almost complete stretching appears which reflects the existence of a nucleation barrier for small globules (a nucleating globule seed for $\tilde{\epsilon} = 2.08$ is highlighted by a broken circle in the snapshots) [17].

The dependence of the force on $\tilde{\epsilon}$ is demonstrated in Fig. 2(a), where we plot the force vs extension profiles for different cohesive strengths at the lowest pulling speed probed in this study. We determine average plateau forces F_p as indicated by horizontal broken lines, which are plotted in Fig. 2(b) for two different chain lengths. Since dissipation is almost negligible at this small stretching velocity, the plateau force F_p corresponds to the equilibrium free energy of globule formation per unit length, which scales as $F_p a/(k_BT) \sim \tilde{\epsilon} - \tilde{\epsilon}_c$ in the collapsed regime. Linear fits to the data in Fig. 2(b) yield the collapse points of $\tilde{\epsilon}_c \approx 0.6 \pm 0.1$ $(N = 50)$ and $\tilde{\epsilon}_c \approx 0.5 \pm 0.1$ $(N = 100)$, in good agreement with previous studies [19].

We now focus on dissipative contributions to the stretching force. The dissipated work is defined as $\Delta W(v, \tilde{\epsilon}) = W(v, \tilde{\epsilon}) - W_{\rm eq}(\tilde{\epsilon})$, where $W(v, \tilde{\epsilon})$ is the velocity-dependent work done during unfolding, and $W_{\rm eq}(\tilde{\epsilon})$ corresponds to the equilibrium work of unfolding a globule, i.e., at $v \to 0$. Figure 3(a) shows force traces upon stretching for different velocities ranging from $\tilde{v} = 0.0045$ to $\tilde{v} = 0.1125$ at fixed cohesive strength. The measured force goes up with increasing velocity due to larger internal friction contributions. The dissipated work is shown in the inset for

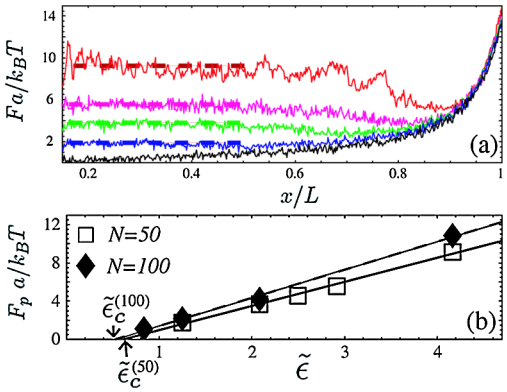

FIG. 2 (color online). (a) Averaged stretching curves for $N = 50$ and different cohesive strengths $\tilde{\epsilon} = 0$, 1.25, 2.08, 2.91, and 4.1 (from bottom to top) at $\tilde{v} = 0.0045$. The dashed lines indicate the fitted plateau force F_p. (b) F_p as a function of $\tilde{\epsilon}$ for two different chain lengths. The lines are linear fits to the data (see text for details).

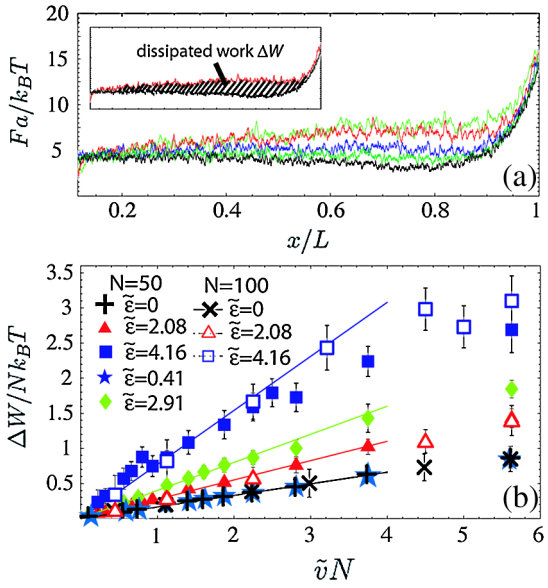

FIG. 3 (color online). (a) Stretching traces for $N = 100$ and $\tilde{\epsilon} = 2.08$ at different pulling velocities $\tilde{v} = 0.1125$, 0.09, 0.045, 0.0225, and 0.0045 (from top to bottom). Inset: The dissipated work ΔW is defined as the area between the top trace (here $\tilde{v} = 0.09$) and the one for $\tilde{v} = 0.0045$. (b) Dissipated work per monomer $\Delta W/(Nk_BT)$ as a function of the rescaled velocity $\tilde{v}N$ for different cohesive strengths $\tilde{\epsilon}$ and N. Linear fits according to Eq. (2) with $\gamma = 1$ yield the internal viscosity η_G.

a given velocity. We note that the work integral is done over the whole length interval studied, i.e., $0.1L < x < L$.

The dissipative work can be written in general as

$$\Delta W = \int_0^L dx \Gamma(v) v, \tag{1}$$

which defines the rate-dependent friction coefficient $\Gamma(v)$ (to simplify notation, we extend the lower boundary of the integral to zero and neglect that two strands are simultaneously pulled out). In what follows, we concentrate on the linear-response regime and neglect any velocity dependence of Γ, as appropriate for low enough pulling speeds (and corroborated by the simulation results). In analogy to Stokes friction of a sphere, we define the friction coefficient to scale as $\Gamma \sim \eta_G a N_G^\gamma$, where η_G is the internal globule viscosity and $N_G \approx (L - x)/(2a)$ corresponds to the number of monomers in the globule. The exponent γ reflects the dissipation mechanism at work during globule dissolution. For local *intensive* dissipation one expects Γ to be independent of N (i.e., $\gamma = 0$), while for global *extensive* dissipation a finite fraction of the globule rearranges during pulling and $\gamma = 1$. The dissipative work follows as

$$\Delta W \sim \eta_G a^2 v N^{\gamma+1}. \tag{2}$$

In Fig. 3(b), we present the dissipation per monomer $\Delta W/(Nk_BT)$ as a function of rescaled velocity $\tilde{v}N$. For small values of $\tilde{v}N$, a few conclusions can be drawn from this scaling plot: (i) All data are linear in the scaling variable $\tilde{v}N$ for fixed N, showing that the friction coefficient Γ is indeed independent of $\tilde{v}$ and our simulations reach the experimentally relevant linear-response regime. (ii) Furthermore, data for different chain lengths superimpose, indicating that $\Delta W/N \sim N$ and thus $\gamma = 1$. We conclude that the dissipation is extensive and involves a finite fraction of the globule. (iii) The data for a phantom chain $\tilde{\epsilon} = 0$ (crosses and plus signs) and for a self-avoiding but noncollapsed chain $\tilde{\epsilon} = 0.41$ (stars) show identical slopes, suggesting that for uncollapsed chains, i.e., $\tilde{\epsilon} < \tilde{\epsilon}_c$, friction due to monomer-monomer attraction and entanglements is negligible in the present simulation protocol. (iv) For $\tilde{\epsilon} > \tilde{\epsilon}_c$, on the other hand, cohesive forces hamper the unfolding and thus enhance the internal viscosity η_G, which according to Eq. (2) follows from the slope of the linear fits in Fig. 3(b). In the noninteracting limit $\epsilon = 0$, the simulated dissipation is solely due to the background solvent viscosity η_0, and we thus expect the total globule viscosity η_G to tend towards η_0 as $\epsilon \to 0$. This allows us to eliminate numerical prefactors from Eq. (2) by writing $\Delta W/\Delta W_0 - 1 = (\eta_G - \eta_0)/\eta_0$, where $\gamma = 1$ and ΔW_0 is the dissipation for $\epsilon = 0$. We plot in Fig. 4 $\Delta W/\Delta W_0 - 1$ as extracted from the linear fits in Fig. 3(b), which thus is a measure of the relative excess internal viscosity. As anticipated, the internal friction only gives a sizable contribution in the collapsed phase. The data for the highest cohesion $\tilde{\epsilon} = 4.16$ in Fig. 3(b) show deviations from the simple scaling at large velocities $\tilde{v}$, which can be traced to the fact that under these conditions the globule relaxation dynamics becomes slower than the externally imposed unfolding cycle, and linear-response theory becomes invalid (see the supplementary information [20]).

To account for the observed behavior, we consider the simplest model for internal friction in a globule: a monomer moving in a corrugated potential created by its neighbors [14]. More quantitatively, one considers a Brownian particle moving in a sinusoidal potential $U_{\text{eff}}(x) = (\theta/2) \times (\epsilon - \epsilon_c) \sin(\pi x/a)$, where x is some suitably chosen reaction coordinate. This corrugated potential mimics the intermonomer cohesion, which disappears at the collapse

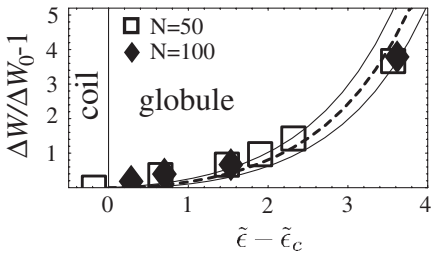

FIG. 4. Rescaled dissipated work, equivalent to the excess internal viscosity $\Delta W/\Delta W_0 - 1 \simeq \eta_G/\eta_0 - 1$, obtained from the linear fits in Fig. 3(b) as a function of the effective cohesive strength $\tilde{\epsilon} - \tilde{\epsilon}_c$. The broken line denotes Eq. (3) with $\theta = 1.125$ and the solid lines the confidence interval due to the error in $\tilde{\epsilon}_c$.

transition, i.e., for $\epsilon = \epsilon_c$, and θ is a fitting parameter. The solution to the one-dimensional diffusion problem in the viscous limit within linear response gives an effective viscosity $\eta_G/\eta_0 = I_0^2(\theta(\epsilon - \epsilon_c)/2k_BT)$ [14], where $I_0(z)$ is the zeroth order modified Bessel function with the limits $I_0(z) \sim 1 + z^2/4$ for $z \ll 1$ and $I_0(z) \sim (2\pi z)^{-1/2}e^z$ for $z \gg 1$. Hence, our final scaling form for the excess internal viscosity follows as

$$(\eta_G - \eta_0)/\eta_0 \simeq I_0^2\left(\frac{\theta(\epsilon - \epsilon_c)}{2k_BT}\right) - 1, \qquad (3)$$

which is shown in Fig. 4 as a broken line with the fitted factor $\theta = 1.125$. This value is very close to 1, implying that the height of the potential is essentially that of the effective cohesive potential $\tilde{\epsilon} - \tilde{\epsilon}_c$, where $\tilde{\epsilon}_c$ has been evaluated independently from Fig. 2(b). The solid lines represent the confidence interval of Eq. (3) due to the error in $\tilde{\epsilon}_c$. As can be seen, the scaling form Eq. (3) is in good agreement with the numerical data for strongly collapsed globules, suggesting a simple exponential dependence of η_G on the effective cohesive strength. This shows that, although the dissipation mechanism is extensive and involves a constant fraction of the globule, the arising friction follows the functional form of a single particle moving in a corrugated potential with an amplitude corresponding approximately to the cohesive energy of a single monomer-monomer bond, clearly an unexpected result. On the other hand, near the collapse transition where our model does not perform as well, we expect that force-induced globule rotation due to topological constraints becomes important and leads to the discrepancies observed in the plot.

Finally, we compare our results with experiments on collapsed DNA [10,21]. The effective internal friction constant was measured to be $\Gamma_{\text{eff}} \approx 10^{-7}$ kg/s for λ-DNA condensed with 400 μM spermidine. Using our result Eq. (2) and the stretching distance $L = 2aN \approx 8$ μm [10], the internal viscosity η_G is obtained as $\eta_G \simeq 2.6 \times 10^{-3}$ kg/m s, and thus $(\eta_G - \eta_0)/\eta_0 \approx 1.6$, where we used the water viscosity $\eta_0 \approx 10^{-3}$ kg/m s. From Fig. 4, we read off an attractive energy $\epsilon - \epsilon_c \sim 2.5k_BT$. That cohesive energy can be directly compared with equilibrium dissolution forces of condensed DNA globules by locating the plateau force of unfolding. From our data [Fig. 2(b)], we find $F_p \simeq 2.9(\epsilon - \epsilon_c)/a$ for $N = 100$. Substituting effective monomer radius (or persistence length), $a \simeq L_p \approx 30$ nm [21] and using $k_BT \simeq 4.4$ pN nm, we predict a plateau force $F_p \approx 1$ pN, which is fairly close to the experimentally reported value $F_p \approx 0.7$ pN [10]. This shows that our treatment of internal globular friction gives a consistent description when compared to the corresponding equilibrium globular dissolution plateau forces of DNA.

In summary, we have presented a general approach to calculate friction coefficients at the single molecule level by directly measuring the dissipated work during unfolding of a polymeric globule. Within the linear-response regime, we show that the internal viscosity outweighs the solvent viscosity already for moderate values of the cohesive strength. The agreement with experimental results for collapsed DNA is promising. We plan to extend our results to the nonlinear regime and to sequence-specific systems such as proteins or RNA.

We thank Y. Murayama for discussions. Financial support from the German Excellence Initiative via the Nanosystems Initiative Munich (NIM) and from MEXT-Japan (No. 20740241) (H. W.) is acknowledged.

[1] M. Rief, M. Gautel, F. Oesterhelt, J. M. Fernandez, and H. E. Gaub, Science **276**, 1109 (1997).
[2] A. Ansari *et al.*, Science **256**, 1796 (1992).
[3] D. Vitkup, D. Ringe, G. A. Petsko, and M. Karplus, Nat. Struct. Biol. **7**, 34 (2000).
[4] D. E. Sagnella, J. E. Straub, and D. Thirumalai, J. Chem. Phys. **113**, 7702 (2000).
[5] P. G. de Gennes, *Scaling Concepts in Polymer Physics* (Cornell University Press, Ithaca, NY, 1985).
[6] B. S. Khatri, M. Kawakami, K. Byrne, D. A. Smith, and T. C. B. McLeish, Biophys. J. **92**, 1825 (2007).
[7] G. S. Jas, W. A. Eaton, and J. Hofrichter, J. Phys. Chem. B **105**, 261 (2001).
[8] M. G. Poirier, A. Nemani, P. Gupta, S. Eroglu, and J. F. Marko, Phys. Rev. Lett. **86**, 360 (2001).
[9] S. A. Pabit, H. Roder, and S. J. Hagen, Biochemistry **43**, 12 532 (2004).
[10] Y. Murayama, H. Wada, and M. Sano, Europhys. Lett. **79**, 58 001 (2007).
[11] G. Hummer and A. Szabo, Biophys. J. **85**, 5 (2003).
[12] A. V. Finkelstein and O. V. Galzitskaya, Phys. Life Rev. **1**, 23 (2004).
[13] Remo Gerber *et al.*, J. Biol. Chem. **282**, 6300 (2007).
[14] R. Zwanzig, Proc. Natl. Acad. Sci. U.S.A. **85**, 2029 (1988).
[15] C. Hyeon and D. Thirumalai, Proc. Natl. Acad. Sci. U.S.A. **100**, 10 249 (2003).
[16] D. K. Klimov and D. Thirumalai, Proc. Natl. Acad. Sci. U.S.A. **96**, 6166 (1999).
[17] T. Frisch and A. Verga Phys. Rev. E **65**, 041801 (2002).
[18] N. Yoshinaga, K. Yoshikawa, and T. Ohta, Eur. Phys. J. E **17**, 485 (2005).
[19] A. Alexander-Katz *et al.*, Phys. Rev. Lett. **97**, 138101 (2006).
[20] See EPAPS Document No. E-PRLTAO-103-015930 for details on the globule dynamics. For more information on EPAPS, see http://www.aip.org/pubservs/epaps.html.
[21] Y. Murayama, Y. Sakamaki, and M. Sano, Phys. Rev. Lett. **90**, 018102 (2003).